Journal of Applied Fluid Mechanics, Vol. 18, No. 9, pp. 2434-2452, 2025.
Available online at www.jafmonline.net, ISSN 1735-3572, EISSN 1735-3645.
https://doi.org/10.47176/jafm.18.9.3301

Heat Transfer Optimization of Three Sections of Mini-channel with CuO Nanofluid

F. H. Ali [1†], Z. H. Saadoon[1], Q. R. Al-amir[2] and H. K. Hamzah[1]

[1] College of Engineering-Mechanical Engineering Department -University of Babylon, Babylon, 51001, Iraq
[2] Mechanical Power Engineering Department -College of Engineering and Technologies-Al-Mustaqbal University, Babylon, 51001, Iraq

†Corresponding Author Email: eng.farooq.hassan@uobabylon.edu.iq

ABSTRACT

Three-dimensional channel designs (rectangular, convergent, and converge-diverge) using distilled water and (CuO) nanofluids as a coolant have been compared numerically and experimentally. The flow rate of coolant, and concentration of volume, with Reynolds number (200≤Re≤1000) and volume fraction (0%≤φ≤7.5%) are applied. The heat flux was provided from below to simulate the operation of a real heat sink, while the rest of the outer surfaces were isolated to compare the optimum performance between three cross sectional areas. To prove the accurateness of the numerical results and the reliability of the program software, a comparison was made between the experimental and numerical outcomes. The wall temperature and average Nusselt number of pure water and nanofluid were chosen as comparison parameters since they represent global parameters. The comparison results showed good coincidence of wall temperature and Nusselt number results for both distilled and nanofluid. According to the results, raising the nano concentration can improve the heat sink's execution and the Nusselt number improved by 38.4% at a volumetric concentration of 7.5%, while the enhancement reaches 10% when varying the form of minichannel. In general, heat transfer is enhanced with increasing Reynolds number for all proposed shapes. In another context, the results of the performance evaluation criteria showed that the convergent channel has the highest value, followed by the convergent-divergent channel, compared to the rectangular channel.

Article History

Received January 21, 2025
Revised April 12, 2025
Accepted April 15, 2025
Available online July 5, 2025

Keywords:

Convergent channel
Heat sink
Mini-channel
Nanofluid
Converge-diverge channel

1. INTRODUCTION

Power engineers have tended to enhance the efficiency of thermal devices as a result of restrictions placed on traditional sources of energy and worries about environmental contamination. During use, these electronic devices generate heat that needs to be continuously removed. As a result, heat sinks are used for this purpose.

Air cooling can be widely used in cooling electronic devices even if the temperature is less than 100°C Because of the poor thermal specification (thermal conductivity and heat capacity).

These systems are incapable of cooling small-scale, fast processors. While liquid-cooled heatsinks outperform air-cooled heatsinks, Researchers have been studying how to enhance the efficiency of these dispersants. Working fluids that have better thermal properties should be utilized instead of traditional ones because they have weak thermal characteristics. Nano fluids, which have a higher thermal conductivity than traditional liquids, are known as nanofluid, therefore, adding nanoparticles enhances the thermal features of the base liquid. Current research has converged on utilizing nanoparticles to enhance heat transfer (Kulandaivel et al. 2024a, b; Farade et al. 2024; Ramasekhar & Jawad 2024; Ramasekhar et al. 2024 and Jawad et al. 2024a,b). Experimental and analytical tests have shown that nanoscale fluids have a higher thermal conductivity than traditional liquids, making them more effective in cooling systems. In the same context, the addition of nanomaterials is not limited to adding them to Newtonian fluids but it also has the same effect in non-Newtonian fluids (Sadiq et al. 2024; Waseem et al. 2024a,b,c).

Nomenclature

A	area	$\dot{x}, \dot{y}, \dot{z}$	Cartesian coordinates
A_S	base area of heat sink	m	mass
A_{th}	area contact of fluid and heat sink	**Greek symbols**	
b	perimeter	μ	dynamic viscosity
C_p	specific heat at constant pressure	ρ	density
D_h	hydraulic diameter	φ	nanoparticle volume fraction
f	friction factor	**Subscripts**	
g	gravitational acceleration	C	channel
h	heat transfer coefficient	f	pure fluid
H_C	channel height	p	solid particles
H	height	nf	nanofluid
k	thermal conductivity	I	inlet
L	length	**Abbreviations**	
Nu	Nusselt number	Conv.	convergent
Δp	pressure drops	Conv.-Dive.	convergent-divergent
p	pressure	DW	distilled water
q_{in}	heat flux	HS	heat sink
Q	overall heat transfer	en	entrance
R_{th}	total thermal resistance	ex	exit
Re	Reynolds number	MCHS	micro_channel heat sink
t_W	channel width	MiCHS	mini_channel heat sink
T	temperature	LC	liquid cooling
T_{Wm}	wall mean temperature	Rect.	rectangular
$\vec{u}', \vec{v}', \vec{w}$	flow velocity	sur	surface
W	width	WF	Working Fluid
W_C	channel width		

Gunnasegaran et al. (2010) conducted a numerical analysis of three channels of various shapes: rectangular, triangular, and trapezoidal microchannel heat sinks using pure water as a coolant. The outcome demonstrated that heat sinks with the smallest hydraulic diameter can achieve the better heat transfer coefficient. Farsad et al. (2011) provided a numerical examination of a copper MCHS (micro_channel heat sink) employing the working fluids (CuO-H_2O, Al_2O_3-H_2O, and Cu-H_2O). The outcome offered that the competence in cooling of an (Al_2O_3-H_2O) nanofluid MCHS (vol 8 percent) is improved by about 4.5% as related with pure water micro_channel heatsinks.

Fazeli et al. (2012) used SiO_2 nanofluid as a coolant to investigate the heat transfer features of the MiCHS (mini_channel heat sink) both experimentally and numerically. A HS (heat sink) consisting of a composition of round canals was used. The numerical findings demonstrated that the height and number of channels, in addition to the channel diameter, had an essential action on the HS's maximum temperature. Their findings showed that using fluid nanoparticles as a LC (liquid coolant) in place of DW (Distilled Water) considerably increased heat transfer and decreased thermal resistance. Ho and Chen, (2013) carried out an experimental work on the cooling effectiveness of an Aluminum Oxide-H_2O nanofluid in a small-channel HS.

Nanofluid heat sinks have a much higher heat transfer coefficient than their pure water counterparts. Experimental research was carried by Sohel et al. (2014) on the thermal implementation of MiCHS utilizing nanofluid (Al_2O3-H_2O) as the coolant instead of distilled water. The outcome displayed that the Nu has grown larger than 18%. The heat sink's basic temperature (around 2.7 °C) was greatly lowered by the nanofluid to DW. The outcomes of this investigation exposed that using nf with DW as a WF (Working Fluid) increased the efficiency of heat transmission. However, it causes the pressure drop to increase. Najafabadi and Moraveji (2016) explored numerically three-dimensional incompressible laminar fluid flow. The results have shown that increasing nanoparticulate volume contributes to an increased Nusselt number and decreases the wall temperature of the heat sink. However, it results in the unwelcome impact of driving power rise and entropy generation. Sakanova et al. (2015) examined the corrugated micro-channel heat sink-filled nanofluid computationally. For a number of nanofluids, the impacts of wavy amplitude, volumetric flow rate, volume percentage, and wavelength were investigated. Their findings showed that, when distilled water is used as the coolant instead of a standard rectangular channel, the efficiency of heat transmission is greatly increased, and that, when nanofluid is used in place of distilled water, the impact of wavy walls is rendered undetectable.

In an experiment by Azizi et al. (2015) to investigate how the thermal efficiency of a cylinder-shaped micro-channel heat sink may be enhanced when Copper-Water nf was utilized as a LC. In contrast to distilled water, the results confirmed that the coefficient of heat transfer of nanofluid increased by roughly (17%), (19%), and (23%) for numerous concentrations of nanofluid (Azizi et al., 2016). They also looked at improvements in heat transfer

coefficients, friction factor, and the local Nusselt number. The outcome revealed the Nusselt number can be improved to 43% while the friction factor enlarged as compared with that of distilled water.

Hasan (2016) compared the enlarged microchannel with straight microchannels and numerically investigated the expanded microchannel. As working fluids, three different nanofluids (Cu-H_2O, diamond-H_2O and Al_2O_3-H_2O) were investigated and their effects on the overall effectiveness of the heat sink were compared to that of pure water. The findings demonstrated that raising the extension ratio or reducing the extension length increases the overall microchannel heat sink efficiency. In a MCHS with a serpentine shape, Sivakumar et al. (2016) examined the efficacy of forced convection heat transfer in (Al_2O_3-water and CuO-water) nanofluids. According to the findings, CuO-water nanofluid has a higher heat transfer coefficient than Al_2O_3-H_2O and dispersed water. To obtain a higher cooling rate and less pumping power by using pure water as a coolant. Zhang et al. (2017) studied numerically the small canal. The consequences demonstrated that the transfer of heat increases with the sum of step stacks as well as that the three-step assembly is the best for heat transfer because of the consequent significant variation in temperature between the liquid flow and canal surfaces.

Abdollahi et al. (2017) analyzed numerically the stream of liquid and the features of heat transmission of the laminar flow of nanofluid in the microchannel heat sink with V-shape inlet-outlet pre-preparation using various nanofluids in distilled water as a base fluid (SiO_2, ZnO, Al_2O_3, and CuO). The outcomes showed that the (SiO_2–H_2O) nanofluid has the maximum rate of Nusselt number in comparison with other studies of nanofluids. Ghasemi et al. (2017) showed a numerical analysis of the impact of Copper Oxide-Water nf on the chilling implementation of 2-shapes heat sinks (circular and rectangular shapes). A comparison's outcome between rectangle and circular canals at the alike Re showed that the HS with Rect. shape has a slighter thermal resistance. Khoshvaght-Aliabadi (2017) investigated a wavy shape HS using rectangular ribs and Aluminum Oxide-Water nf. The pressure drop and heat transfer coefficient of the ribbed-wavy heat sinks were higher than those of the smooth-wavy sinks, according to the results. In order to evaluate the heat transmission rate and laminar liquid flow in a Rect. MCHS provided with cable twist insertions; Feng et al. (2017) completed a computational investigation. The findings demonstrated that the longitudinal vortices of the wire coils significantly increased the efficiency of heat transmission in the MCHS where the performance factor increases and ranges between 1.4-1.8 if the wire is long and placed in the middle of the channel.

Tang et al. (2017) have presented a new dual-film heat sink. The outcomes of their investigation demonstrate that the dual-film construction promotes heat exchange in both orientation (horizontal & vertical), resulting in a temperature distribution that is equal throughout and excellent heat transfer efficiency. Ghani et al. (2017) studied heat transfer augmentation by numerical model of a MCHS with wavy enclosures over a Reynolds range between 100-800. The results showed that the highest performance factor was found at highest Reynolds number. The geometrical optimization can be used to increase heat transmission with a low pressure drop in a microchannel that has rectangular ribs and sinusoidal cavities. The study determined that the ideal values for relative cavity amplitude, rib width, and rib length were, respectively, 0.15, 0.13, and 0.5. When compared to other designs that were investigated, the combination of these ideal values produced the highest performance factor. The thermal and heat transfer coefficients decrease with increasing Re values. Naphon et al. (2018) investigated three methods for enhancing heat transfer: jet impingement, nanofluid, and micro-channel heat sink. The outcome results show that an 18.56% heat transfer enhancement could be achieved at a concentration of 0.015%. Furthermore, the obtained heat transfer coefficient tends to rise as nozzle diameter and nozzle level height are reduced. Saeed and Kim (2018) conducted experimental and numerical study for three different channel shape with Al_2O_3 nanomaterials. They discovered that compared to pure water, nanofluids have a much greater convective heat transfer coefficient, also, the numerical outcomes of the 2-phase method were in near contract with experimental results, while the results of single-phase approach were less. Experimental research on the laminar movement and heat transfer specifications of pure water inside a helical minichannel cylindrical HS was conducted by Falahat et al. (2019). Their consequences displayed that raising the Reynolds number and reducing the channel helix angle augment heat transmission from the heat sink. Besides, pressure drops as the Reynolds number rises and the helix angle falls as the Reynolds number rises and the helix angle falls.

The surface temperature, heat removed, power consumption, thermal resistance, and electronic chip reliability were numerically analyzed by Kumar and Kumar (2020). They showed that the Nusselt number is rising and that the dependability of electronic chips is increased by 70% when utilizing nanofluid as a cooling in place of just distilled water. Muhammad et al. (2019) investigated how different nanofluids (Al_2O_3, SiO_2 and Cu) embedded in distilled water with concentration (0-0.8%) affected pressure drop and heat transmission in the (dive. _conv.) small channel, it shows slight change in pressure load with different fluid concentrations. They showed that the hydrothermal presentation of the heat sink can be enhanced by using nanofluid and diverging-converging minichannel. Experimental research on the heat transmission and hydro-dynamic properties of TiO_2-water nanofluid used as a coolant in three different wavy channels heat sinks was conducted by Sajid et al. (2019). The results showed that addition of nanomaterials improve heat transfer for all different shapes of mini-channel heat sink. The flow of polyalkylene–glycol–TiO2 non-Newtonian nanofluids in elliptical microchannels was examined by Ragueb and Mansouri (2023). The analysis's findings demonstrated that both the aspect ratio and the Brinkman number had a significant impression on the temperature distribution. Furthermore, when compared to the circular microchannel, the elliptical microchannel

demonstrated a notable improvement in the amount of heat transfer and a reduction of half in thermal length. For all heat sinks, the findings illustrated that nanofluids had better heated transfer capabilities than pure water. Abdulqadur et al. (2019) offered an innovative design includes a hybrid mini-channel that starts straight and then transforms into a wavy channel, which provides increased heat sink are with lowest possible pressure drop. The results showed that innovative mini-channel is highly effective in reducing the maximum temperature and achieving uniform temperature distribution. Kahani (2020) studied mathematically the thermal efficacy of Aluminum Oxide nf flow over a HS. The results demonstrated that decreasing the dimension of np raises the Nu. The biggest increases in the Nusselt number, of around 38%, were observed at Reynolds 100 for (1%), volume concentration of nanofluid flow. Tariq et al. (2020) have quantitatively explored the impact of slab width on the overall effectiveness of the MiCHS. The findings showed that the heat transfer reduced while the temperature at base and pressure drop increased when the slab thickness in the mini_channel heat sink grew from 0.2 to 1.6 mm. A heat sink's hydraulic and thermal efficiency was numerically evaluated by Naranjani et al. (2021).

Their research demonstrated that using wavy channels improves heat transmission by (24–36%) compared to conventional channels, although pumping power requirements increase by (20–31%), leading to a 16–24% gain in total performance. Tahiri et al. (2024) reported a numerical study of entropy due to heat transfer, fluid flow and magnetic field in laminar regime through a micro_channel. The findings show that the highest generation of entropy occurs at the highest values of magnetic field (Ha) and a dimensionless parameter arising from the formulation (η) obtained for ($\phi = -1$). Additionally, the rate of local generation of entropy in the entrance regions are maximum close the channel surfaces.

Heidarshenas et al. (2020) conducted an experiment to ascertain the impact of different alumina nanoparticle sizes on the coefficient of heat transmission in a HS with cylindrical micro channel. Their studies showed that the convective heat (Nusselt number) reduces as nano size rises. The heat transmission and pressure difference in a MiCHS using (Al_2O_3–H_2O and TiO_2-H_2O) nanofluids have been experimentally considered by Moghanlou et al. (2020). The consequence showed that the (TiO_2-H_2O) was too composed to establish a 4.56% improvement in the heat transmission. Numerical study by Hadavand et al. (2019) conducted the mixed laminar convection in semicircular shape with lid-driven. Silver water nanofluid is a coolant used to cooling the electronic chip, study focused on the effect of the angle of attack on heat transfer and skin friction, so many of angle of attack were studied, 90o, 45o, 0o, -45o and -90o. The results of the study showed that increasing the angle of attack above 0° leads to decrease in the Nusselt number and surface friction. In a magnetohydrodynamic (MHD) fluid flow, Ragueb et al. (2023) examined heat transmission and entropy formation in a micro_channel exposed to discrepancy heating, viscous dissipation, and Joule heating. The average Nusselt (Nu) for both plates converge to twice channels when the Hartmann number (Ha) is low and one plate is heated while the other is cooled, according to the results. Nevertheless, there was an 8% discrepancy between the two plates' Nu values at high Ha values that considered viscous dissipation and Joule heating, with the cooling plate having the higher Nu. Al-Mohsen et al. (2021) investigated numerical approach of cylindrical heat sink using finite element formulation based Galerkin approximation. The study concentrated on augmentation heat transfer on laminar flow by augmenting the heat dissipation area by making the surface of the cylindrical heat sink corrugated. Two parameters controlled by the surface corrugations are the number of corrugations and amplitude which can increase the heat transfer dissipation reach to 20.47% with copper oxide nanoparticles. Saadoon et al. (2022, 2023) conducted a numerical solution for the rectangular straight channel with a flat and wavy inner surface. Different types of nanofluid of nanoparticles such as iron oxide, alumina, titanium oxide and silver which add to pure water to boost thermal conductivity of working fluid. Also, convergent-divergent cross-sectional channels were examined and compared with straight channel heat sinks. The Reynolds number ranges between 200-1000 which represents the laminar flow regime. Their results show that heat transfer enhanced with wavy and convergent-divergence which reached 54% at high Reynolds number and concentration of nanofluid. According to Ghani et al. (2017), geometrical optimization can be used to increase heat transmission with a low pressure drop in a microchannel that has rectangular ribs and sinusoidal cavities. The study determined that the ideal values for relative cavity amplitude, rib width, and rib length were, respectively, 0.15, 0.13, and 0.5. When compared to other designs that were investigated, the combination of these ideal values produced the highest performance factor. The thermal and heat transfer coefficients decrease with increasing Re values. The heat transfer and pressure drop properties of MCHS with a 1 mm hydraulic diameter were examined by Arshad and Ali (2017). Distilled water and TiO2 are used as the coolant for analysis at powers of 100, 125, and 150 W.

Nusselt number and heating power are unrelated when using distilled water as a coolant; on the other hand, TiO2 nanofluid performs better at lower heating powers. Kumar et al. (2022) created a branching, wavy channel when using Al2O3 Nanofluids as working fluids for Reynolds numbers ranging from 100 to 300. The secondary flow and macroscopically mixing were improved by this arrangement. In comparison to a straight channel, there was a 154% increase in heat transfer with a 2% volumetric concentration of nanofluids at a Reynolds number of 30.

The literature review mentioned above indicates that the channel shape and coolant type have a significant impact on the rate of heat transmission in a MiCHS. From reviewing the previous literature, it is clear that there are many studies that have addressed improving heat transfer in mini-channels by adding nanomaterial or changing the cross-section of the channel individually. Therefore, this

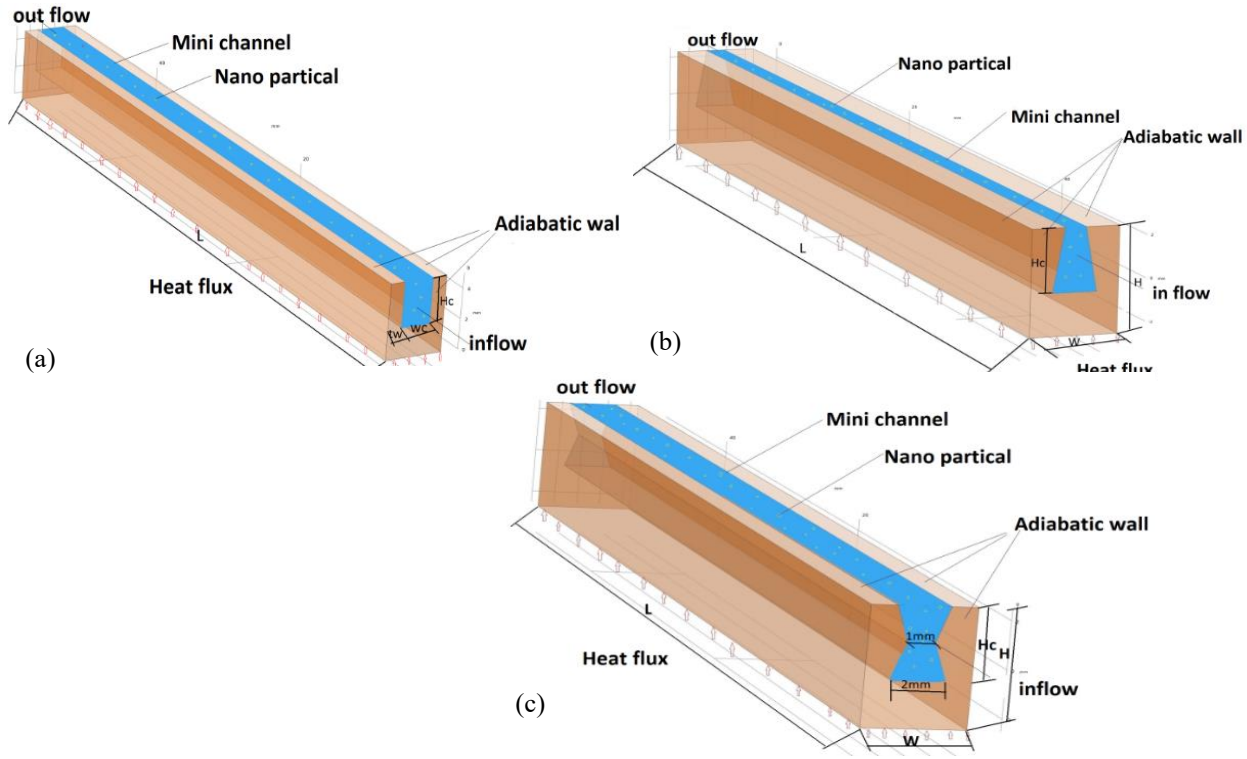

Fig. 1 Schematic diagram of the present problem(a) rectangular (b) convergent (c) converge-diverge channel

study presented the idea of combining them. In the present work an experimental and numerical investigation for three-dimensional minichannel heat sink of the three different cross-sectional areas with nanofluids using (COMSOL program) which is based finite element techniques. The study compared the (CuO-H_2O) nanofluid and DW as a LC for various volume concentrations and various flow rates, and investigated the effects of varying the cross-sectional form of the MiCHS (converge, converge-diverge and rectangular) on the heat transfer and fluid flow and comparison with rectangular cross section. The study aims to enhance heat transfer through two features: adding nanomaterial at different concentration and changing the cross-sectional area of the mini-channel (converging, converging-diverging). The main objective of this study is to improve the design of miniature cooling systems in thermal applications, such as cooling electronic processors or solar panels, and to determine the extent to which heat transfer is improved when using. In addition to knowing how the channel shape affects the cooling efficiency and flow resistance. The effect of nanofluid concentration, channel cross-sectional shape, and Reynolds number were discussed. In Previous experimental or numerical studies, the current designs (convergent, convergent-divergent) were not studied, so the current study is the first study to analyze flow and heat transfer in these forms of mini-channel.

2. PHYSICAL MODEL DESCRIPTION, GOVERNING EQUATION AND NUMERICAL SOLUTION APPROACH

Figure 1 shows the physical models utilized in the numerical study. As a starting point, the Rect. MiCHS is employed. It has one channel and is constructed of copper. The dimensions of a rectangular mini-channel are as: 1mm for the wall thickness (t_W), 2 mm for the channel width (W_C), 3 mm for the channel height (H_C), and 5 mm for the heat sink height (H). According to Fig. 1(a), the bottom surface receives a heat flux of 180 KW/m2 and is 4 mm (W) × 50 mm (L) in size. Fig.1 (b) show the convergent channel heat sink, which has the same dimensions as the rectangular channel, but we made a modification on the walls of the channel (sloping at an angle of 10° degrees inward with vertical axis). The rectangular channel shape underwent another modification, which resulted in the converge- diverge pattern shown in Fig. 1(c), by narrowing the channel's center by 1 mm. The area of different shapes (rectangular, convergent and convergent-divergent) are (0.0024 m^2, 0.019741m^2 and 0.002m^2 respectively). Table 1 shows the dimensions symbols and their value for three mini-channels.

Table 1 Symboles and dimensions of case study

Symbol	L	H_C	H	W	W_C	t_W
Dimension (mm)	55	3	5	4	2	1

The shape of cross sectional of mini-channel plays an effective role in enhancing heat transfer within the channel, as it can increase the exterior area of contact between the fluid and the mini_channel surface. Some of cross_sectional shape can also transform the flow from a laminar to a turbulent flow inside the mini-channels passages. In the current study, two new heat sink shapes (convergent, convergent-divergent) are designed and

compare with common rectangular cross-section. The goal of these two designs is to reduce the pressure drope and enhanced fluid structure to remove heat.

2.1 Assumption and Governing Equations:

Several assumptions regarding a mini channel's operating state have been made to simplify the analysis in this paper which are: the fluid flow in three-dimensional is steady, incompressible, Newtonian, obeys to the law of Poiseuille, single phase and laminar. Constant thermophysical properties of the solid, the fluid thermophysical properties are varying piecewise-linear with fluid temperature, the surface of mini-channel heat sink is adiabatic. The gravitational force other body forces and viscous dissipation are insignificant. Radiation is considered to be an insignificant form of heat transmission. As for the nanomaterials, it is considered homogenous, single-phase approach.

The main equation for this prototypical is as follows, built on the presumptions indicated above: Continuity equation for coolant Feng et al. (2017):

$$\frac{\partial \vec{u}'}{\partial \dot{x}} + \frac{\partial \vec{v}'}{\partial \dot{y}} + \frac{\partial \vec{w}'}{\partial \dot{z}} = 0 \tag{1}$$

Momentum equations in cartesian coordinates given as

$$\vec{u}'\frac{\partial \vec{u}'}{\partial \dot{x}} + \vec{v}'\frac{\partial \vec{u}'}{\partial \dot{y}} + \vec{w}'\frac{\partial \vec{u}}{\partial \dot{z}} = -\frac{1}{\rho}\frac{\partial p}{\partial \dot{x}} + \frac{\mu}{\rho}\left(\frac{\partial^2 \vec{u}'}{\partial \dot{x}^2} + \frac{\partial^2 \vec{u}'}{\partial \dot{y}^2} + \frac{\partial^2 \vec{u}'}{\partial \dot{z}^2}\right) \tag{2}$$

$$\vec{u}'\frac{\partial \vec{v}'}{\partial \dot{x}} + \vec{v}'\frac{\partial \vec{v}'}{\partial \dot{y}} + \vec{w}'\frac{\partial \vec{v}'}{\partial \dot{z}} = -\frac{1}{\rho}\frac{\partial p}{\partial \dot{y}} + \frac{\mu}{\rho}\left(\frac{\partial^2 \vec{v}'}{\partial \dot{x}^2} + \frac{\partial^2 \vec{v}'}{\partial \dot{y}^2} + \frac{\partial^2 \vec{v}'}{\partial \dot{z}^2}\right) \tag{3}$$

$$\vec{u}'\frac{\partial \vec{w}'}{\partial \dot{x}} + \vec{v}'\frac{\partial \vec{w}'}{\partial \dot{y}} + \vec{w}'\frac{\partial \vec{w}'}{\partial \dot{z}} = -\frac{1}{\rho}\frac{\partial p}{\partial \dot{y}} + \frac{\mu}{\rho}\left(\frac{\partial^2 \vec{w}'}{\partial \dot{x}^2} + \frac{\partial^2 \vec{w}'}{\partial \dot{y}^2} + \frac{\partial^2 \vec{w}'}{\partial \dot{z}^2}\right) \tag{4}$$

Where $\vec{u}'$, $\vec{v}'$ and $\vec{w}'$ represent the velocity components in $\dot{x}$, $\dot{y}$ and $\dot{z}$ directions, respectively. Also, p, ρ and μ represent the pressure, density and dynamic viscosity of the coolant (DW or nf), respectively. The energy equations for the LC are as follows:

$$u'\frac{\partial T_f}{\partial \dot{x}} + v'\frac{\partial T_f}{\partial \dot{y}} + w'\frac{\partial T_f}{\partial \dot{z}} = \frac{k_f}{\rho c_p}\left(\frac{\partial^2 T_f}{\partial \dot{x}^2} + \frac{\partial^2 T_f}{\partial \dot{y}^2} + \frac{\partial^2 T_f}{\partial \dot{z}^2}\right) \tag{5}$$

The following is the form of the energy equation for the solid domain:

$$k_s\left(\frac{\partial^2 T_s}{\partial \dot{x}^2} + \frac{\partial^2 T_s}{\partial \dot{y}^2} + \frac{\partial^2 T_s}{\partial \dot{z}^2}\right) = 0 \tag{6}$$

The T (temperature) and k_f (thermal conductivities) of DW and nf, respectively, are T_f and T_s, k_f and k_s.

2.2 Boundary Conditions

The following boundary conditions are defined in order to explain the aforementioned mathematical equations for the computing field:

- Coolant fluid temperature is (293K) at the input.
- Pressure at the outlet is imposed with 0 Pa which refers to atmospheric pressure which considered as reference pressure.
- A constant heat flux of 180 KW/m^2 was applied to the bottom wall.
- On any of the outside surfaces, there was no heat loss.
- At the inlet the velocity corresponds to the Reynolds number variety from 200 to 1000, where $\vec{u}'=\vec{u}'_{in}$, $\vec{v}'=0$, $\vec{w}'=0$.
- At the mini-channel wall-coolant interface $\vec{u}'=0$, $\vec{v}'=0$, $\vec{w}'=0$, and $q_{convection}=q_{conduction}$. $-k_f\frac{\partial T_f}{\partial n} = k_s\frac{\partial T_s}{\partial n}$

2.3 Reduction of Data

The hydraulic diameter (D_h) and Reynold number (Re) are definite as follows Feng et al. (2017):

$$D_h = \frac{4A}{b} = \frac{4W_cH_c}{2(w_c+H_c)} = \frac{2W_cH_c}{(W_c+H_c)} \tag{7}$$

$$Re = \frac{\rho \vec{u}'_{in}\, Dh}{\mu} \tag{8}$$

Where ρ, $\vec{u}'_{in}$, and μ are the density, inlet velocity of the fluid, and dynamic viscosity respectively. W_c and H_c are the width and height of the mini-channel, respectively. The total thermal resistance (R_{th}), the friction factor (f), and the pressure difference (Δp) between the inlet and outlet of the mini_channel heat sink are calculated by Feng et al. (2017):

$$R_{th} = \frac{T_{max}-T_{in}}{Q} \tag{9}$$

$$f = \frac{\Delta p D_h}{2\rho \vec{u}'^{\,2}_{in} L} \tag{10}$$

$$\Delta p = p_{in} - p_{out} \tag{11}$$

Where: L denotes the length of the mini channel, p_{in} and p_{out} are static pressure at the inlet and outlet of MiCHS, T_{max} and T_{in} are the maximum temperature of a mini channel and the fluid temperature at inlet, respectively. Q denotes the overall heat transfer and is given by ($Q = q_{in}A_s$); where q_{in}: represent the heat flux applied at the base of heat sink; As: The base area of a HS and is stated by ($A_s=W_c \times L$). The Nusselt number"Nu" is evaluated by Feng et al. (2017):

$$Nu = \frac{Q\, D_h}{k_f\, A_{th}(T_{wm}-T_f)} \tag{12}$$

Where T_{Wm} is mean heat sink temperature, T_f is the average temperature of working fluid, A_{th} is the contact surface area of working fluid and the base area of heat sink, k_f is the fluid thermal conductivity.

2.4 Thermophysical Characteristics of Fluids

The distilled water and (CuO-H_2O) nano-fluid with volume fractions of (0.025,0.05 and 0.075) are used in the present study as coolant. Table 2 illustrates the thermophysical-properties of nanoparticles. Since the temperature difference as a result of heat flux does not rise to the range that affected the properties of the coolant fluid.

Table 2 Thermophysical properties of nanoparticles Sakanova et al. (2015) and Heidarshenas et al. (2019)

Property	Density (kg/m^3)	Specific heat (J/kgK) water	Thermal conductivity (W/mK)
CuO	6500	535.6	20
Distilled water	997.1	4179	0.613

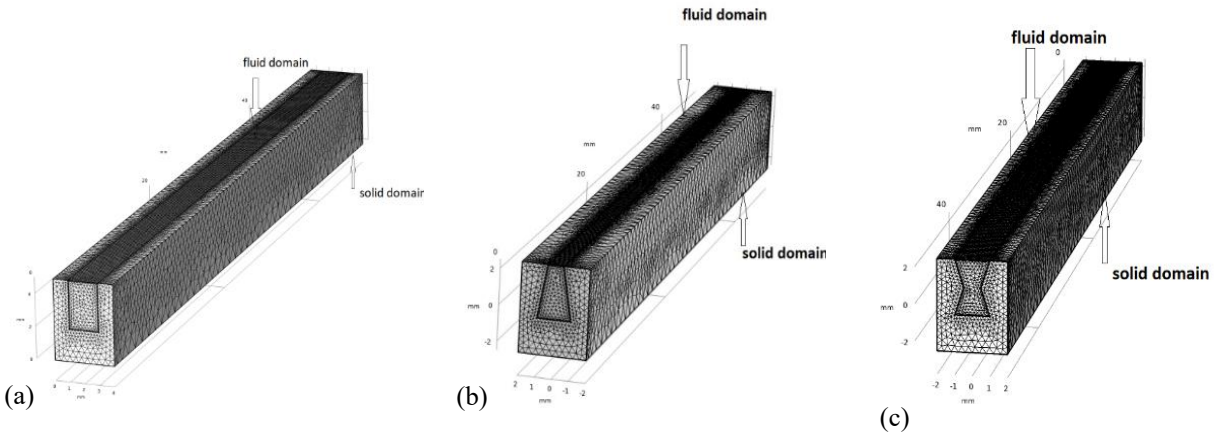

Fig. 2 Mesh distribution of the computational domain (a) Rectangular, (b) Convergent, (c) Converge- Diverge channel

The thermophysical properties of nanofluid were assessed using the next equations. Using the model developed by Sakanova et al. (2015), the density and specific heat of nanofluid were calculated.

$$\rho_{nf} = (1-\varphi)\rho_f + \varphi\rho_p \tag{13}$$

$$cp_{nf=} \frac{\varphi(\rho cp)_p + (1-\varphi)\rho_f cp_f}{\rho_{nf}} \tag{14}$$

Using the Hamilton & Crosser model, the thermal conductivity of the nanofluids is calculated Hamilton & Crosser (1962):

$$k_{nf=} \frac{k_p + (n-1)k_f - (n-1)\varphi(k_f - k_p)}{k_p + (n-1)k_f + \varphi(k_f - k_p)} k_f \tag{15}$$

Where n is constant and equal to 3 for spherical shape nanoparticles.

The μ (dynamic viscosity) of nf is determined using the model of Brinkman (1952):

$$\mu_{nf} = \frac{\mu_f}{(1-\varphi)^{2.5}} \tag{16}$$

Where nanoparticle concentration, heat capacity, thermal conductivity, viscosity, and density are denoted by φ, C_p, k, μ, and ρ, respectively. While the subscripts f, p, and nf, respectively, stand for base fluid, nanoparticle, and nanofluid.

2.5 Mesh Sensitivity and Validation

Grid generation testing in computational fluid dynamic is essential to obtain accurate results, because the computational model contains many equations that are solved in a complex way, it is liked to a freely distribution grid for both the liquid field and the solid field, taking into account that the grid should have a high density in the contact areas between the liquid and the solid. The grid consists of a structured network of tetrahedron elements. To reduce the effect of grid roughness on the accuracy of the results, the grid independence is tested by taking a case from the study cases and applying different forms of grids to reach accurate results. This method is applied in many previous numerical studies, like Feng et al. (2017). Figure 2 shows the free grids distributions for three different mini-channels. A grid independence exam was achieved to certify that the correct numerical findings. A grid independent test was conducted for four meshes in order to determine the appropriate mesh size, labelled as (extra fine), (finer), (fine) and (normal) with number of elements 7820763, 1876205, 570155 and 222511 respectively. The maximum temperature (T_{max}) and Nusselt number for a rectangular mini-channel heat sink were calculated for each mesh, and the results are compared at a Reynolds number of 400 and a heat flow of 180 kW/ m^2. The virtual inaccuracy of the selected variables was calculated using the formula below Ghani et al. (2017).

$$\mathrm{E}(\%) = \left| \frac{B_2 - B_1}{B_1} \right| \times 100 \tag{17}$$

Any variables, such as (pressure drops, friction factor, the Nusselt number, or temperature) is denoted by (B). The variables values obtained from the optimum grids and other grids are denoted by B1 and B2, respectively. Variables such as Nusselt number, maximum temperature were chosen and the error percentage adopted in the solution because these variables are global and comprehensive parameters. The extra fine mesh with the quickest run time while maintaining mesh independence is presented in Table 3. Because high smoothness has the lowest error for both Nusselt number and the maximum temperature, it was chosen to obtain results.

Table 3 Mesh sensitivity test for rectangular mini channel heat sink at Re=400, q = 180 kW/m^2

Element Size	Domain element	Nu	Nu error%	T_{max}(K)	T_{max} error%	Friction factor	Friction factor error%
extra fine	7820763	15.211	1.42%	343	2.62%	0.064	-4.47%
Finer	1876205	14.994	17.3%	334	1.79%	0.067	-5.63%
Fine	570155	12.394	18.83%	328	0.304%	0.071	-8.97%
Normal	222511	10.060	-	327	-	0.078	

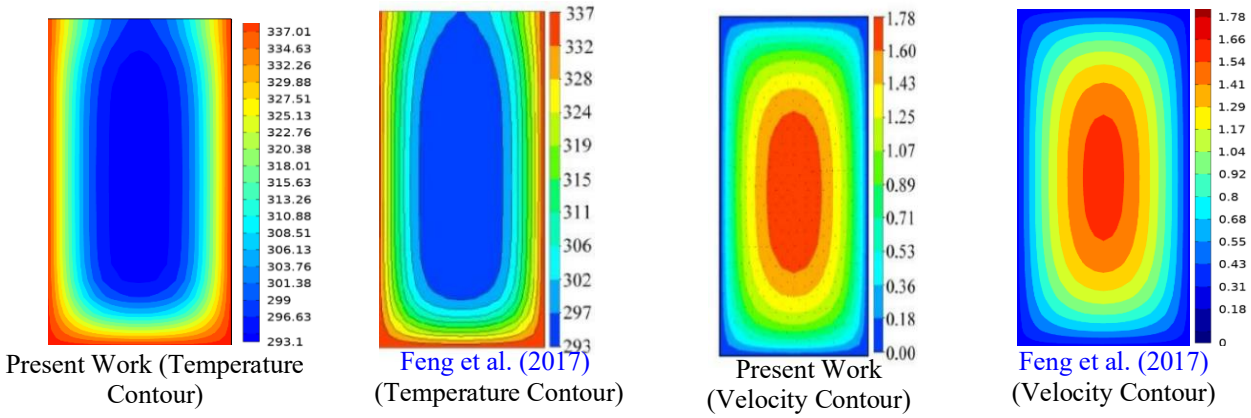

Present Work (Temperature Contour) | Feng et al. (2017) (Temperature Contour) | Present Work (Velocity Contour) | Feng et al. (2017) (Velocity Contour)

Fig. 3 Temperature and Velocity contours comparison between present work and Feng et al. (2017) on a cross section (x/L=0.625) in microchannel at Re=663 and q=400 kW/m^2

To verify that numerical results are accurate. particularly considering that this study is the first to employ the finite element method-based COMSOL Multiphysics code. Simulation models are compared in contrast to prior computational investigations. The validation model is compared to Feng et al. (2017) who used the program ANSYS CFX to examine the coupled heat transfer rate and laminar fluid flow in the rectangle micro-channel heat sink equipped with wire coil insertions. The comparison between the current COMSOL simulations and the published computations is shown in Figs. (3) and (4) for the absent wire coil instance. Strong agreement between the two approaches is observed. To ensure the accuracy and reliability of the present study, validation was agreement between the two approaches is observed. To ensure the accuracy and reliability of the present study, validation was performed by comparing results with the experimental and numerical data from Feng et al. (2017).

This study was selected based on the following key criteria:

1. Relevance to Mini-Channel Heat Transfer
2. Matching Key Parameters for Comparison
3. Reliability of Selected Studies
4. Close to geometry, boundary conditions and working fluid.

In the existing study, the numerical solution was carried out using the COMSOL Multiphysics tool to resolve the three-dimensional problem dealing with heat transmission and fluid movement within a mini-channel. Numerous engineering applications use the CFD module

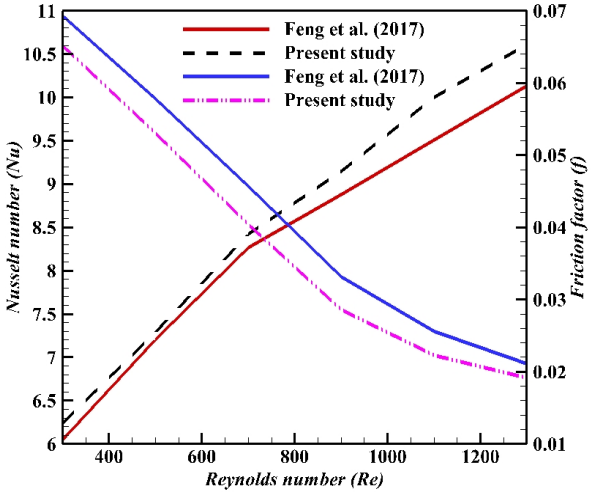

Fig. 4 Validation with Feng et al. (2017) by comparison of Variation of *Nusselt number* and *Friction factor* with *Reynolds number*.

to comprehend how fluid and heat transfer behave in various occurrences. The broad competencies of the CFD module include two- and three-dimensional steady and unsteady fluid and heat transfer problems. In COMSOL Multiphysics, a CFD module based on the finite element technique is used to explain the partial differential equations for two fields (solid and fluid) that regulate the problem region. In this code, the terms (finite element method) and (Galerkin approach) were used to discretize partial differential equations involving pressure, temperature, and velocity. For tackling CFD problems, a weighted residual approach using Galerkin finite elements was quite effective.

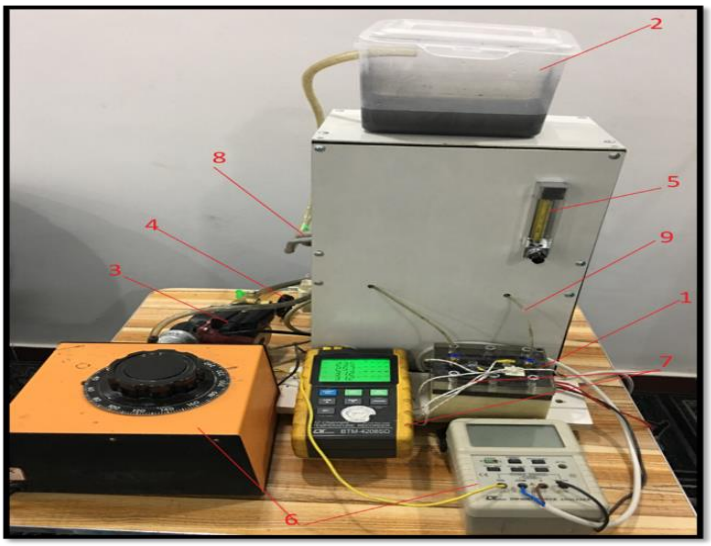

Fig. 5 Experimental rig

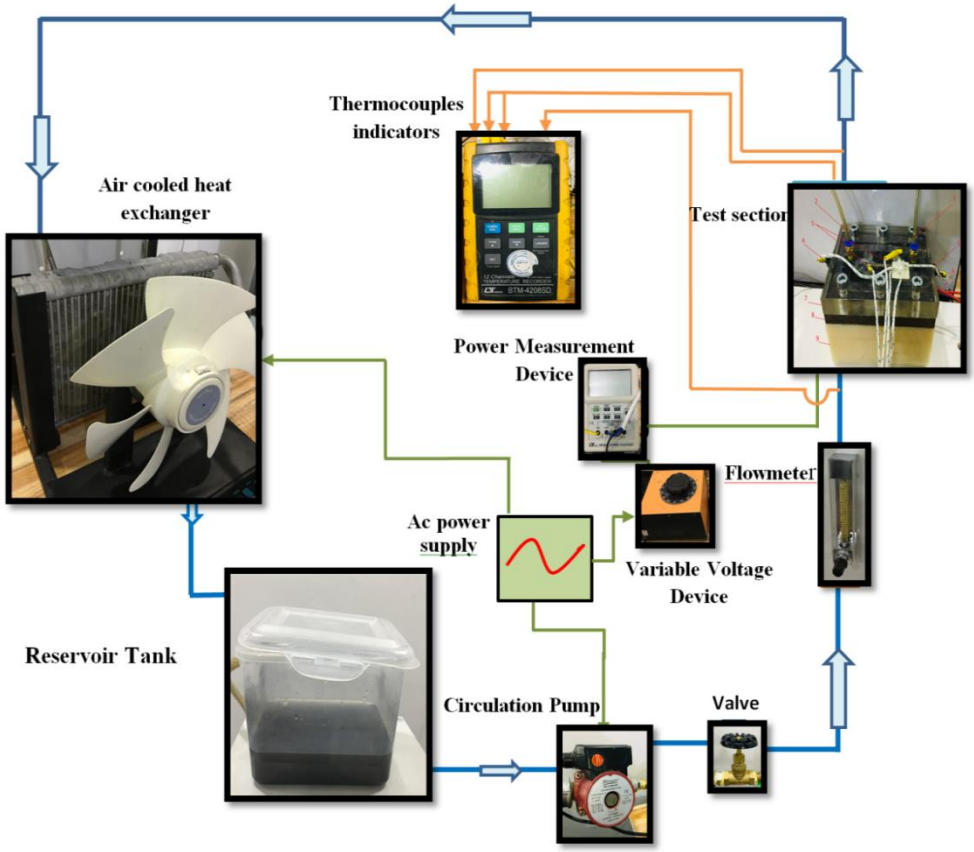

Fig. 6 Device's extensive schematic

3. EXPERIMENTAL DETAILS AND UNCERTAINTY ANALYSIS

Figure 5 shows the test rig's order in all of its components: (1) Test section; (2) Storage tank; (3) Pump; (4) Globe valve; (5) Flow meter; (6) Power supply system; a-Digital Power Analyzer, b-Voltage regulator; (7) Temperature measuring device: a-Digital temperature recorder, b- Thermocouple type K; (8) Small air-heat exchanger; (9) Conveying tube. The detailed schematic for the device is exhibited in Fig. 6. The apparatus having two parts: the test section and test loop.

3.1 Test Section

A copper mini-channel heat sink is located in the test section. It is shaped by a method of wire cutting machinery. At the base of a HS, a constant heat flux is given. In this respect, a cylinder heater is placed in a cube made of copper and it fitted in perforation that bored inside of a cube, every side of a cube was thermally isolated by polytetrafluoroethylene excepting the upper side that had

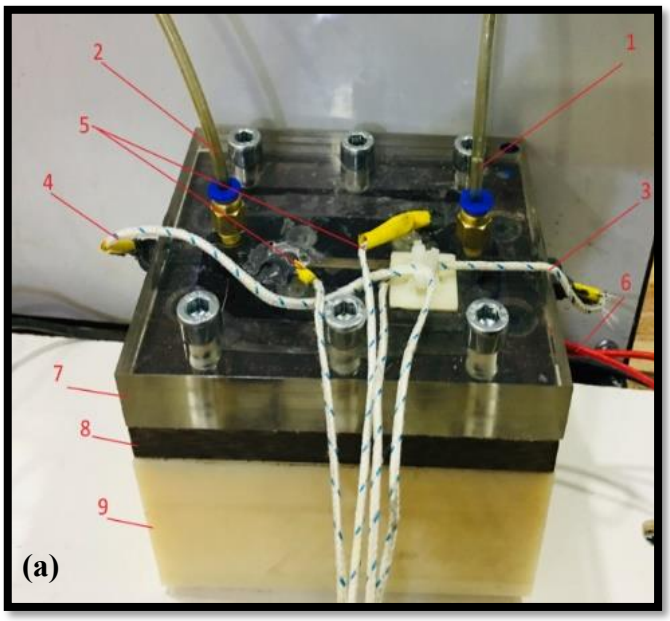

1- Fluid entry area

2- Fluid exit area

3- Thermocouple (T_{en})

4- Thermocouple (T_{ex})

5- Thermocouple (T_{sur})

6- Heater

7, 8- Plexiglass sheets

9- Polytetrafluoroethylene

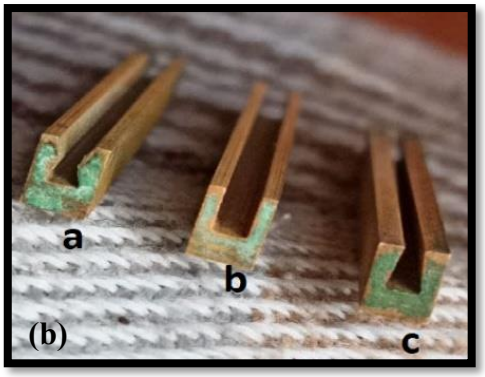

a-converge-diverge section

b-rectangular section

c- convergent mini section

Fig. 7 (a) the test section and (b) the channels of heat sink

touched with the base of a MiCHS. A translucent acrylic cover with (10 mm) thick enclosed the upper region of the heat sink and it is firmly fixed to guarantee no leakage occurs while the pump is on. The transparent cover contains two holes for the entry and exit of a working fluid, two holes for the thermocouples for measuring the heat sink temperature and two side holes for the thermocouples for measuring the inlet and outlet temperature of the fluid, as shown in Fig.7.

3.2 Test Loop

The test loop consists of a test section, working fluid storage tank, a small heat exchanger, pump to circulate the fluid through the test ring, and flowmeter to measure the fluid flow, where contains a control valve in addition to the control valve installed after the pump, through which it is possible to control the rates of the pump through which it is determined. The flow corresponds to the Reynolds number (400, 600, and 1000). The coolant fluid is circulated from the tank by the pump along the tubes through the MiCHS where the heat is absorbed from the MiCHS and thus the temperature of fluid increases and then flows in the direction of the heat exchanger where the heat is dispersed into the atmospheric to obtain the required temperature at the entrance to the test section 293K. Thus, it returns to the closed-loop system. The fluid temperatures at the entrance and exit as well as the heat sink wall temperature are measured using four thermocouples.

3.3 Procedure for Testing

Multiple experimental tests were carried out to study the effect of changing the channel's shape (rectangular, converge, and converge-diverge) as well as using the nanofluid in place of pure water as a coolant for different flow rates (0.06,0.09,0.15) lpm corresponding to the Reynolds number (400,600,1000) on the general performance of the mini channel heat sink as follows:

1- The pump is switched on and the flow is adjusted to the required value for each condition using the control valve.

2-By using the voltage controller, to provide the required temperature, the cylinder heater is regulated.

3- After the fluid discharges from the test section, it will enter the heat exchanger to cool it and return it to the tank.

4- Two thermocouples were installed at the heat sink wall temperature and another two thermocouples were installed at the fluid entry and exit regions.

5-The above steps are repeated in other cases.

Table 4 Specifications of ultrasonic cleaner bath

Model	JTS-1018
Tanks working dimension (mm)	L= 406; W=305; H=460
Overall dimension (mm)	L= 586; W=485; H=680
Ultrasonic frequency	40 Khz
Ultrasonic power	720 W
Digital timer control	1-30 min
Capacity	54 L
Temperature control range (ºC)	< 90 ºC
Ultrasonic power output	800 W

Table 5 Experimental and empirical measurement results of density and viscosity

Density ρ (kg/m^3)		Dynamic viscosity μ (N.s/m^2)	
Experimental result	Empirical result	Experimental result	Empirical result
1403.4	1409.8	0.001151	0.0012152

3.4 Preparation of Nanofluid

The nanofluid preparation step is considered one of the very important steps for its decisive effect on the stability of the nanoparticles in the base fluid. In the current work the following steps were taken to prepare the (CuO-H_2O) nanofluid with a volume fraction (0.075):

1-The weight of the nanoparticles required for (2 liters) of pure water was calculated to prepare the nanofluid with a

volume concentration of (0.075) according to the following equation by Sajid et al. (2019).

$$\varphi = \frac{\left(\frac{m_p}{\rho_p}\right)}{\left(\frac{m_p}{\rho_p}\right)+\left(\frac{m_f}{\rho_f}\right)} \tag{18}$$

2- The required amount of powder was weighed by a sensor balance.

3- The np were disordered with DW in a magnetic stirrer for an hour to ensure the dispersal of the nanoparticles and prevent their accumulation, and after that, the mixture was placed for 6 hours in a cleaned ultrasonic bath which uses ultrasound.

4- Then the nanofluid is ready for the required tests and experiments.

The specifications of ultrasonic cleaner baths are listed in table 4.

The density measurement test was performed by weighing a specific volume of nanofluid using a sensitive balance, where the process was repeated several times to obtain more accurate results. By dividing the measured mass by the volume of the nanofluid, the density value is obtained.

Viscosity is the amount of a fluid's resistance to flow and the amount of resistance to pressure that forces it to move where it is; the higher the viscosity of a fluid, the less its ability to flow.

The viscometer type [Brookfield digital viscometer model DV– III ULTRA], in (The board of industrial R & D - Petrochemical Research Center -Ministry of Science and Technology) was used to measure the viscosity of (CuO-H_2O) nanofluid. The operational theory of a viscometer is that a spindle is rotated through a calibrated spring (which is immersed in the specimen).

The spring deflection is calculated by the viscous nanofluid drag in contravention to the spindle deflection. A rotary transducer provides a torque signal for the spring deflection. The results of experimental measurements of density and viscosity of (7.5%CuO-H_2O) nanofluid are given in table 5. There was a little difference in the density and viscosity measurements with the empirical relation using by Sakanova et al. (2015) and Brinkman model, Brinkman (1952) respectively.

3.5 Performance Evaluation Criterion (*PEC*)

The combined influence of Nusselt number (Nu) and friction factor (f) was employed while analyzing the overall hydro_thermal manner of a small channel using the Performance Evaluation Criterion (PEC) as specified in Eq. 19 Naranjani et al. (2021).

$$PEC = \frac{(Nu_C/Nu_R)}{(f_C/f_R)^{1/3}} \tag{19}$$

Where the subscripts (R and C) depict the HS with a Rect. and (conv., conv.-dive.) MiCHS

Using Kline (1963), it was calculated how uncertain the test result was. Quantities like Wall's temperature and the temperature of the fluid bulk were initially estimated for this determination. Following that, each parameter's error was used to estimate doubts.

Uncertainty is calculated using equation (20) Sadegh Moghanlou et al. (2020).

$$UR = \left[\left(\frac{\partial R}{\partial x1}\,u_1\right)^2 + \left(\frac{\partial R}{\partial x2}\,u_2\right)^2 + \cdots + \left(\frac{\partial R}{\partial xn}\,u_n\right)^2\right]^{0.5} \tag{20}$$

The examples of the uncertainty calculations for the temperature readings as follows:

$$UT_W = \left[\left(\frac{\partial T_W}{\partial T_{W1}}u_{T_{W1}}\right)^2 + \left(\frac{\partial T_W}{\partial T_{W2}}u_{T_{W2}}\right)^2\right]^{0.5}$$
$$= [0.115974 + 0.1263]^{0.5} = 0.49^oC$$

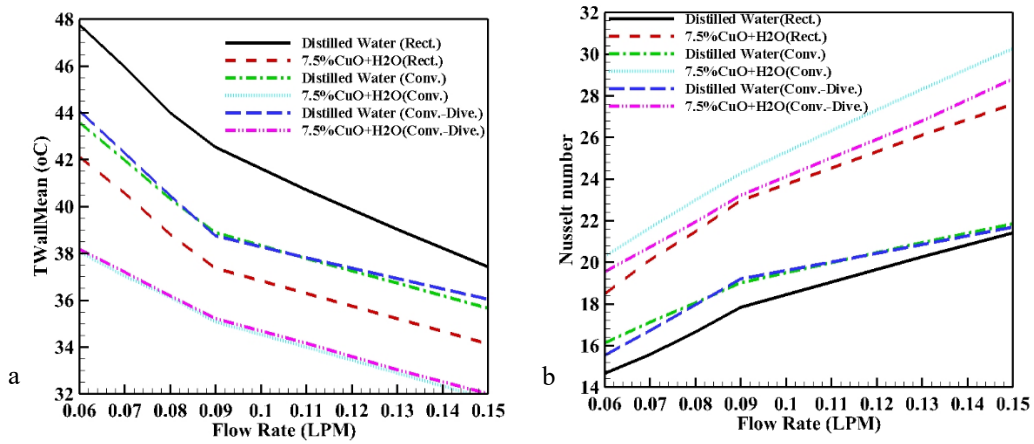

Fig. 8 Effect of using (7.5%CuO+H₂O) nanofluid as a coolant in three different channels. a) Wall mean temperature, b) Nusselt number

$$UT_f = \left[\left(\frac{\partial T_f}{\partial T_{in}}\, u_{T_{in}}\right)^2 + \left(\frac{\partial Tf}{\partial T_o}\, u_{T_o}\right)^2\right]^{0.5} = [0.09954 + 0.1024]^{0.5} = 0.45^o C$$

The uncertainty of the supplied power is calculated as follows:

$$UQ = \left[\left(\frac{\partial Q}{\partial I}\, u_I\right)^2 + \left(\frac{\partial Q}{\partial V}\, u_V\right)^2\right]^{0.5} = [0.10296 + 0.1029]^{0.5} = 0.45\, W$$

Fractional uncertainty=1.4%.

4. RESULTS AND DISCUSSION

4.1 Experimental and Numerical Results

Practical experiments were carried out for three different mini channels (rectangular, convergent, and converge-diverge) using pure water and the (CuO-water) nanofluid as a coolant with volume concentration (0.075) for different flow rates (from 0.06 to 0.15 LPM) and subjected to isoflux (180 kW/m2) at the base. Also calculated the Nusselt number (Nu) and measured thermophysical properties for nanofluid such as density and viscosity. A constant heat flux is delivered at the bottom of a heat sink. The current study included adding CuO nanoparticles to distilled water, and the concentration of the particles ranged from 0 to 7.5%, as these particles have unique thermal and rheological properties Sadegh Moghanlou et al. (2020). CuO nanoparticles have high thermal conductivity and thus contribute effectively to enhancing heat transfer, 14.1% reduction in base temperature was achieved when using CuO with water compared to pure water by Tariq et al. (2019). Figure 8 show the effect of flow rat on both the mean wall temperature of the heat sink (in the figures on the left) and Nusselt number (in the figures on the right) for the three types of mini-channels for the cases distilled water and nanofluid with concentration of 0.075. As for the mean wall temperature, it decreases with increasing flow rate from 0.06 LPM to 0.15 LPM and adding nanoparticles. It can also be observed that the Nusselt number increases with increasing flow rate and the addition of nanomaterials. Increasing the flow rate leads to reducing the thickness of the boundary layer, which increases the heat transfer rate. Adding nanomaterials enhances the thermal conductivity of the working fluid, which also leads to enhanced heat transfer.

All of the channels exhibited the same response, which was a drop in the HS's mean temperature and a rise in the Nu. When comparing the three types of mini-channels, it can be notice that the convergent channel shows the lowest mean temperature and the highest Nusselt number value at all flow rates. This indicates that this channel provides a higher heat exchange compared to the rectangular and convergent-divergent channels.

In this section the numerical results of a convection heat transfer process in MiCHS using pure water and (CuO-H₂O) nanofluid are presented. The study was conducted by looking at four Reynolds numbers (400, 600, 800 and 1000) and a volumetric fraction (0.075).

To verify a simulation model (CFD), the numerical results were compared with the experimental results on three channels under identical organizational and technological conditions. The temperature of the wall for all mini-channels was measured experimentally for different flow rates by using distilled water and nanofluid (7.5%CuO + H₂O) as a coolant and compared with the numerical results, a good match was obtained where the error rate ranged from (0.5-4.2) % when using pure water as a coolant and ranges from (0.78-5.57) % when using the nanofluid as a coolant. Figure 9 & Fig. 10 show the validation between experimental and numerical outcomes of the Nu of three different MiCHS (rectangular, convergent, converge-diverge) for different four Reynolds number (400, 600, 800 and 1000) using pure water and (7.5%CuO+H₂O) nanofluid as a coolant.

These figures demonstrate that when Reynolds number rise Nusselt number rises. A similarity in behavior and a clear convergence was observed, as the maximum deviation between the experimental and numerical values of Nusselt number was from (2.3-12) %. The difference between the experimental and numerical results was due to the experimental uncertainty, the numerical simulation hypotheses, some experimental errors, the accuracy of the instruments and the laboratory conditions.

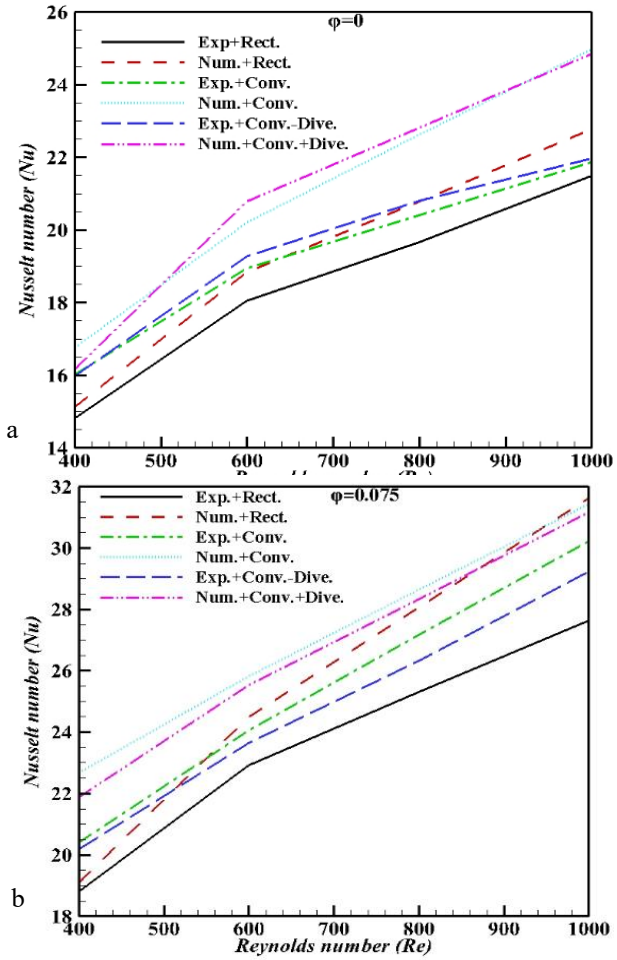

Fig.9 Comparisons between numerical and experimental results of the Nusselt Number for three different mini-channels heat sinks for a) φ=0, b) φ=0.075

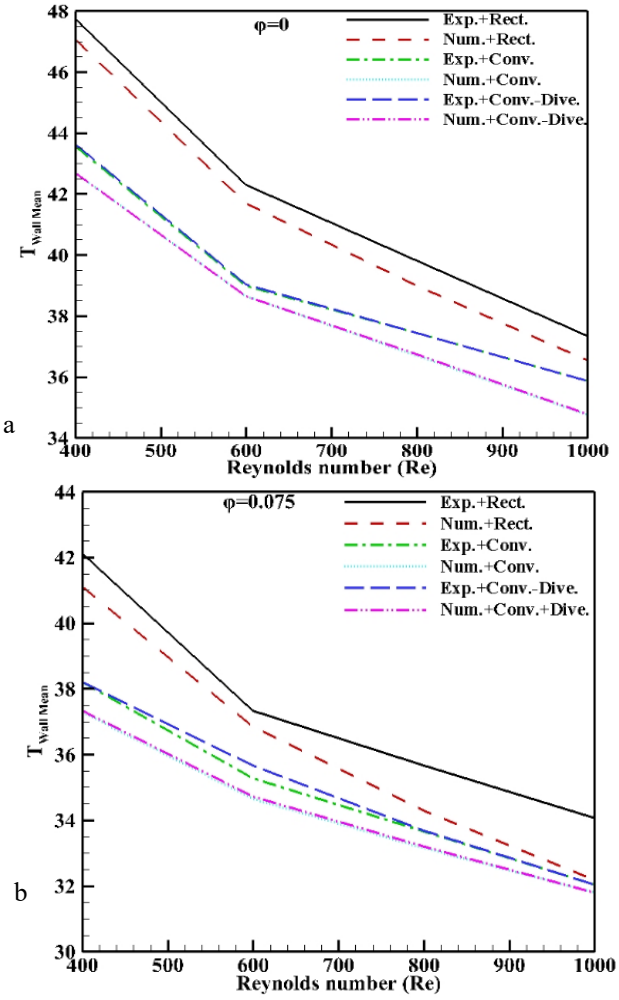

Fig. 10 Comparisons between numerical and experimental results for temperature wall mean for three different mini-channels heat sinks for a) φ=0, b) φ=0.075

In the same context, the temperature wall mean of the base heat sink was compared between the experimental results obtained from measuring the temperature along the channels through the temperature sensors (thermocouples) and the results obtained by numerical simulation in the same positions corresponding to the sensors connected in the practical part. In general Fig. 10 appears that the temperature decreases with increasing Reynolds number as a result of increasing the amount of mass coolant. It also shows acceptable approval between the experimental and numerical outcomes for all types of mini-channels and in the cases of pure water and nanofluid, as the error percentage did not exceed 10% in all cases.

4.2 Hydro_thermal performance features of the mini channel

The heat and flow distribution within the MiCHS should be considered because they have a direct effect on the cooling efficiency.

At Re=1000 and (0.075CuO+H2O) as a nanofluid, Fig. 11 depicts the velocity contours at the exit section and along the MiCHS for three distinct channel shapes (Rec., Conv., and Conv.-Dive.). It appears from this figure that the velocity was augmented by varying the cross section of the mini channel, reaching (0.61, 0.69, 0.72 m/s) in the rectangular, converge-diverge, and convergent mini channels, respectively. This velocity was caused by the reduction in hydraulic diameter produced by the change in channel area and perimeter.

To show the temperature distribution along the mini channel heat sink selected, nanofluid percentage (0.075) under the identical inlet conditions (Tin=293K) and (Re =1000) as shown in Fig.12 The temperature increases along the y-direction from the inlet of the channel to the outlet for different shapes of the channels. Due to the greatest temperature variance between the channel and the temperature of inlet fluid, the mini channel heat sink dissipates heat most efficiently near the inlet. The amount of heat transfer depends on how much the surface and fluid temperatures differ from one another, with the highest heat transfer occurring at the stream's beginning because the fluid's temperature is reduced and the temperature difference is high, which improves the heat transmission from the wall surface to the cool fluid. As an outcome, convection is used to transport heat from the surface to the fluid down the stream.

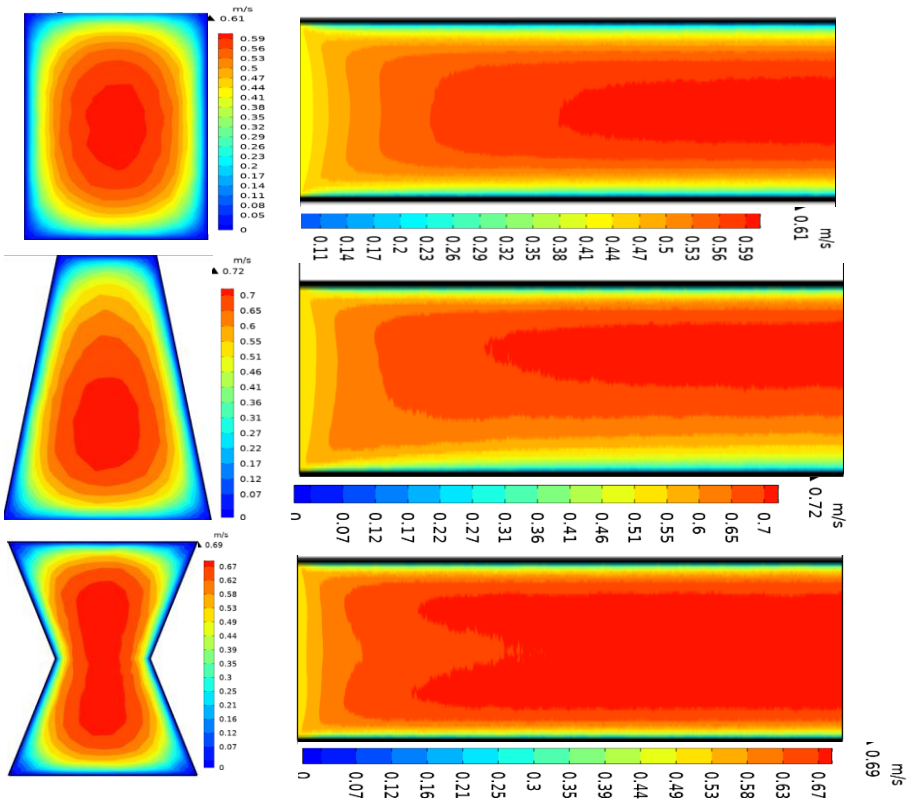

Fig. 11 Velocity contour for the different shape mini channel at Re=1000 and used (7.5% CuO+H_2O) as a coolant.

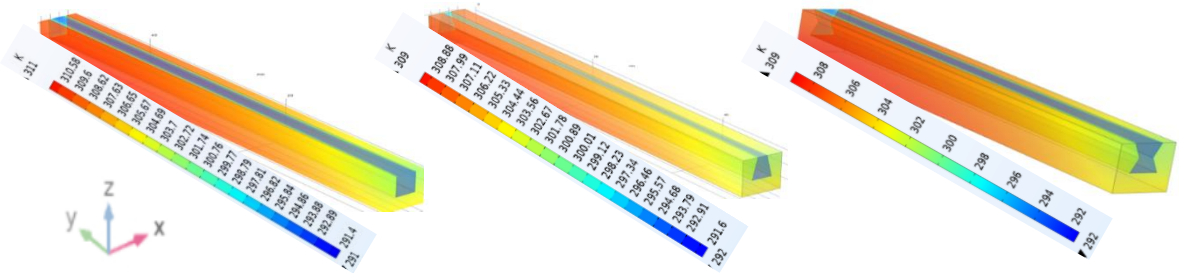

Fig. 12 Temperature contour for the different shape mini channel at Re=1000 and used (7.5% CuO+H_2O) as a coolant.

4.3 Nusselt Number (Nu), Friction Factor (f) & Thermal Resistance (R_{th})

The Nusselt number on the hot surface, which displays the rate of heat transmission from the walls in a non-dimensional formula, is a crucial quantity. Heat transmission rates increase with increasing Nusselt number values. The impact of altering the form of the minichannel on the heat transfer rate was investigated using distilled water as a coolant. Figure 13 demonstrates that the Nusselt number for both convergent and converge-divergent channels (convergent, converge-diverge) is higher than that for the rectangular channel due to the change in hydraulic diameter brought on by the difference in the area and circumference of the channels, which results in a small pressure drop in the larger hydraulic diameter and a lower flow rate pushed into the heat sink. Channels with smaller hydraulic diameter generally provide higher heat transfer coefficients. The

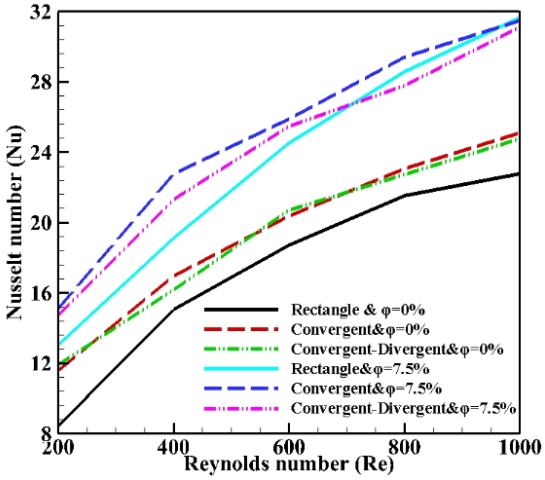

Fig. 13 Effect of using (CuO-H_2O) nanofluid as a coolant on Nusselt number for different channels

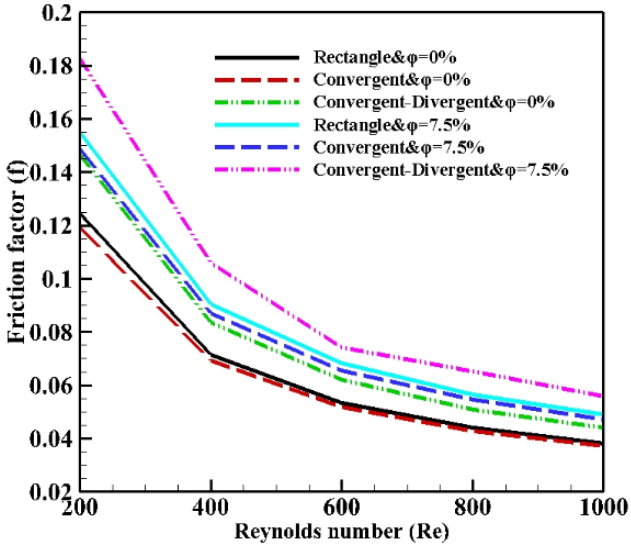

Fig. 14 Effect of using the nanofluid (CuO-H_2O) as a coolant on the friction factor for different channels

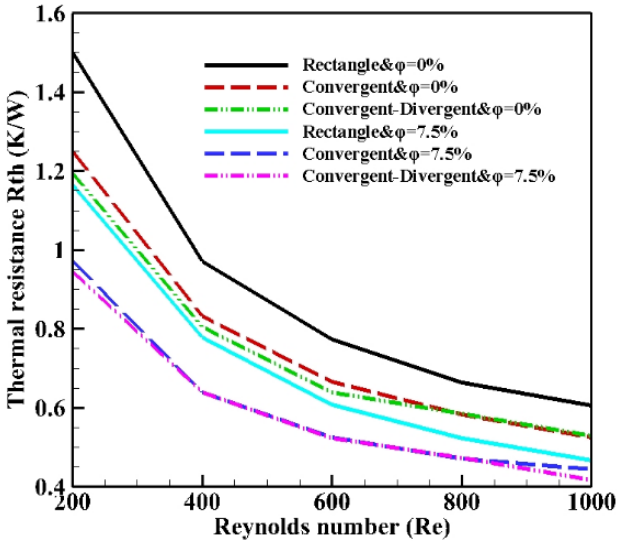

Fig. 15 Effect of using the nanofluid (CuO-H_2O) as a coolant on thermal resistance for different channels

proposed cross-section shapes (convergent, convergent-divergent) enhance the flow acceleration and approach the turbulent flow inside the channel compared to the conventional channel (rectangular). Figure 13 shows the influence of utilizing (CuO-H_2O) nanofluid as a coolant with different volumetric concentrations for different channels. The Nusselt number (Nu) can be seen that rises with the rise of Re. The reason behind the rise in the Nusselt number with the rise in the Reynolds number is the effect of the reducing the thickness of the boundary layer, which results in higher heat absorption from the channel walls. This illustrates that the high entry speed can improve the cooling performance of the heat dispersants as noted that the Nusselt Number (Nu) is higher for the nanofluid compared to pure water and rises with the rise in the nanoparticles percentage because nanoparticles have higher thermal conductivity, thus increasing the thermal conductivity and this ability increases with the increase in the concentration of nanoparticles to increases the participation of nanoparticles in the thermal conductivity. The trends of the curves are similar, and the convergent channel shows higher values of Nusselt number, followed by the convergent-divergent channel, and then the rectangular channel for all Reynolds number and all concentrations.

The effect of fluid velocity (Re) and nanoparticle concentration on the friction factor are appeared in Fig. 14 for three different types of mini-channel. The friction factor is affected by utilizing the nanofluid (CuO-H_2O) as a working fluid, due to the presence of nanoparticles in the nanofluid, which produce an increase in the fluid's viscosity and density, it rises with an increase in volumetric fraction and falls with a rise in Reynolds number. This causes the friction factor to rise while falling with an increase in the Reynolds number since the velocity and friction factor are inversely related. When comparing the friction factor values for three channels, it can be noted that the convergent-divergent channel shows the lowest friction factor values due to the sloping shape of the channel, which provides a simpler flow path,

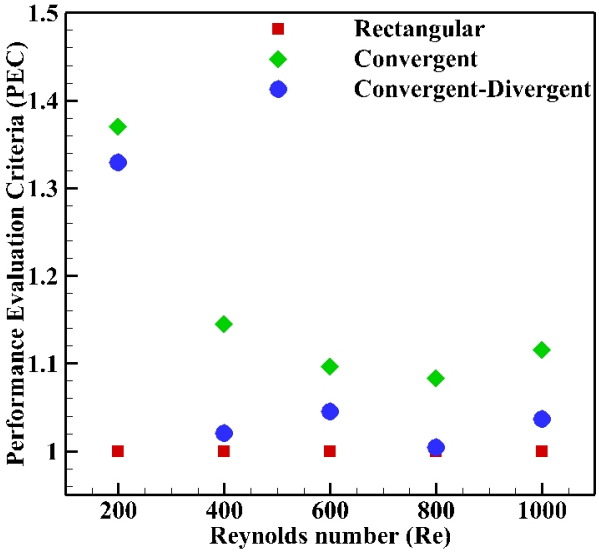

Fig. 16 Variation of PEC versus Reynolds number for pure water as a coolant

followed by the convergent channel and then rectangular channel.

An important parameter through which it refers to the mini_channel heat sink efficiency, as its demonstrations the quality of the thermal performance and the minimum thermal resistance relates to the best mini channel heat sink cooling efficiency. Figure 15 shows that the thermal resistance values with Reynolds number for different concentrations (φ=0, 0.025, 0.05 and 0.075) and three types of mini-channels (rectangular, convergent and convergent-divergent). The thermal resistance decreases as the Reynolds number and nanoparticles concentrations increases. It can be noted that the minimum values of thermal resistance for convergent-divergent channel, while convergent channels having higher values and rectangular channel having highest values.

Figure 16 depicts the difference of the *PEC* as a function of Reynolds number for a small channel with

pure water as the coolant. PEC is a dimensionless number, it represents the ratio of the improvement of the Nusselt number values for the new cross-sectional area (convergent, convergent-divergent channel) to the Nusselt number for the rectangular cross-sectional divided by the ratio of the friction coefficient for the new cross-section (convergent, convergent-divergent) to the friction coefficient for the rectangular cross section as explained by Eq. 19. PEC represents the overall efficiency of the new channels (convergent, convergent-divergent) compared to the regular channel (rectangular channel). This analysis makes it clear that the *PEC* values are larger than one across the board for all Reynolds numbers. The figure shows the disparity of the *PEC* with Reynolds number for a heat flux of 180 kW/m^2 and distilled water as the working fluid, demonstrating the effectiveness of the new designs. It is clear the PEC values are greater than one for the two proposed sections and for all Reynolds values, compared to the standard section (rectangular), which has a PEC of one. The figure also shows the variation in the PEC with the Reynolds number, where it has the highest values at the lowest Reynolds number and decreases with increasing Reynolds number until it reaches 800 and then starts increasing at a Reynolds of 1000. This variation is a result of the changing effect of the cross-section on the flow velocity inside the channel on both sides of heat transfer and the friction factor. However, the convergent channel shows higher PEC than the convergent-divergent channel for all Reynolds values due to flow acceleration and turbulence effect.

5. CONCLUSIONS, STUDY LIMITATION AND FUTURE WORKS

To improve heat transfer, the features of the mini channel heat sink with nanofluid (CuO) as the working fluid and three cross sectional areas were investigated utilizing experimental and numerical techniques in the present study. The numerical simulation model and experimental findings were compared, and it was found that there was strong agreement between them in terms of trends and values, with 12% being the most extreme variation. In this analysis, several flow rates were utilized to look at the coolant's thermal resistance, the heat sink's base temperature, the friction factor, and the Nusselt number. The essential conclusions are drawn:

- The (convergent and converge-diverge) mini channel heat sink with the (CuO-H_2O) nanofluid with volume fraction (φ=0.075) as a coolant at Reynolds number 1000 produced the lowest mean wall temperature of 31.5 °C. By accelerating the flow rate and utilizing nanofluids, it was discovered that the mean wall temperature may be lowered.
- When the Reynolds number was augmented to 1000, the mean temperature dropped to 36.5 °C from the highest measured value of 63.5 °C for a rectangular micro channel heat sink at a Re equal to 200. By utilizing CuO-water nanofluids, it was further reduced by 12.32%.
- By using nanofluids instead of pure water as the working fluid, the thermal resistance values decrease as the volumetric percentage of the nanoparticles increases.
- The Nusselt Number is larger for the nanofluid compared to pure water and increases with the increase in volumetric concentration because nanoparticles have higher thermal conductivity, the rapid entry speed can enhance the cooling process of the heat dispersants.
- The contribution of adding CuO to enhance the Nusselt number was 38.4%, while the contribution of varying the shape of the mini-channel was 10%.
- Heat transfer is improved by growing the Reynolds number values as is known, and the effect of varying the form of the mini-channel from rectangular cross section to convergent and convergent-divergent cross section is more significant for distilled water.
- The highest increase in PEC is at Reynolds value of 200 (PEC=1.37 for convergent & PEC=1.33 for convergent-divergent) while the lowest PEC is at Reynolds values of 800 (PEC=1.08 for convergent & PEC=1.004 for convergent-divergent).
- The PEC values for the convergent cross section are higher than the convergent-divergent cross section for all values of Reynolds number.

There are many challenges that the study faced, the most important of which are the process of manufacturing mini-channel, controlling the flow and reaching a steady state, adding nanomaterial and avoiding the sedimentation state, etc.

The most important research direction that can be recommended are the use of grooves of different shapes along the mini-channel, the use of hybrid nanomaterials, the addition of porous media to the wall of the mini-channel, or studying the effectiveness of using phase change materials.

CONFLICT OF INTEREST

The authors declare that they have no known competing financial interests or personal relationships that could have appeared to influence the work reported in this paper.

AUTHORS CONTRIBUTION

Zahraa H. Saadoon: Writing-original draft, Conceptualization, Data curation, Equalization. **Farooq H. Ali:** Writing-review, Editing, Investigation, Methodology, Resources. **Qusay Rasheed Al-Amir:** Supervision, Methodology. **Hameed K. Hamzah:** Validation, Software, Formal analysis.

REFERENCES

Abdollahi, A., Mohammed, H. A., Vanaki, S. M., Osia, A., & Haghighi, M. G. (2017). Fluid flow and heat transfer of nanofluids in microchannel heat sink with V-type inlet/outlet arrangement. *Alexandria Engineering Journal*, *56*(1), 161-170. https://doi.org/10.1016/j.aej.2016.09.019

Abdulqadur, A. A., Jaffal, H. M., & Khudhur, D. S.

(2019). Performance optimiation of a cylindrical mini-channel heat sink using hybrid straight–wavy channel. *International Journal of Thermal Sciences*, *146*, 106111. https://doi.org/10.1016/j.ijthermalsci.2019.106111

Al-Mohsen, S. A. A., Abed, I. M., & Ali, F. H. (2021). A numerical comparison of circular and corrugation heat sink for laminar CuO–water nano-fluid flow and heat transfer enhancement. *Applied Nanoscience*, 1-28. https://doi.org/10.1007/s13204-021-02003-2

Arshad, W., & Ali, H. M. (2017). Experimental investigation of heat transfer and pressure drop in a straight minichannel heat sink using TiO2 nanofluid. *International Journal of Heat and Mass Transfer*, *110*, 248-256. https://doi.org/10.1016/j.ijheatmasstransfer.2017.03.032

Azizi, Z., Alamdari, A., & Malayeri, M. R. (2015). Convective heat transfer of Cu–water nanofluid in a cylindrical microchannel heat sink. *Energy Conversion and Management*, *101*, 515-524. https://doi.org/10.1016/j.enconman.2015.05.073

Azizi, Z., Alamdari, A., & Malayeri, M. R. (2016). Thermal performance and friction factor of a cylindrical microchannel heat sink cooled by Cu-water nanofluid. *Applied Thermal Engineering*, *99*, 970-978. https://doi.org/10.1016/j.applthermaleng.2016.01.140

Brinkman, H. C. (1952). The viscosity of concentrated suspensions and solutions. *The Journal of Chemical Physics*, *20*(4), 571-571. https://doi.org/10.1063/1.1700493

Falahat, A., Bahoosh, R., Noghrehabadi, A., & Rashidi, M. M. (2019). Experimental study of heat transfer enhancement in a novel cylindrical heat sink with helical minichannels. *Applied Thermal Engineering*, *154*, 585-592. https://doi.org/10.1016/j.applthermaleng.2019.03.120

Farade, R. A., Wahab, N. I. B. A., Mansour, D. E. A., Junaidi, N., Soudagar, M. E. M., Rajamony, R. K., & AlZubaidi, A. (2024). A review on ultrasonic alchemy of oil-based nanofluids for cutting-edge dielectric and heat transfer oils. *Journal of Molecular Liquids*, 125312. https://doi.org/10.1016/j.molliq.2024.125312

Farsad, E., Abbasi, S. P., Zabihi, M. S., & Sabbaghzadeh, J. (2011). Numerical simulation of heat transfer in a micro channel heat sinks using nanofluids. *Heat and Mass Transfer*, *47*(4), 479-490. https://doi.org/10.1007/s00231-010-0735-y

Fazeli, S. A., Hashemi, S. M. H., Zirakzadeh, H., & Ashjaee, M. (2012). Experimental and numerical investigation of heat transfer in a miniature heat sink utilizing silica nanofluid. *Superlattices and Microstructures*, *51*(2), 247-264. https://doi.org/10.1016/j.spmi.2011.11.017

Feng, Z., Luo, X., Guo, F., Li, H., & Zhang, J. (2017). Numerical investigation on laminar flow and heat transfer in rectangular microchannel heat sink with wire coil inserts. *Applied Thermal Engineering*, *116*, 597-609. https://doi.org/10.1016/j.applthermaleng.2017.01.091

Ghani, I. A., Kamaruzaman, N., & Sidik, N. A. C. (2017). Heat transfer augmentation in a microchannel heat sink with sinusoidal cavities and rectangular ribs. *International Journal of Heat and Mass Transfer*, *108*, 1969-1981. https://doi.org/10.1016/j.ijheatmasstransfer.2017.01.046

Ghasemi, S. E., Ranjbar, A. A., & Hosseini, M. J. (2017). Numerical study on effect of CuO-water nanofluid on cooling performance of two different cross-sectional heat sinks. *Advanced Powder Technology*, *28*(6), 1495-1504. https://doi.org/10.1016/j.apt.2017.03.019

Gunnasegaran, P., Mohammed, H. A., Shuaib, N. H., & Saidur, R. (2010). The effect of geometrical parameters on heat transfer characteristics of microchannels heat sink with different shapes. *International Communications in Heat and Mass Transfer*, *37*(8), 1078-1086. https://doi.org/10.1016/j.icheatmasstransfer.2010.06.014

Hadavand, M., Yousefzadeh, S., Akbari, O. A., Pourfattah, F., Nguyen, H. M., & Asadi, A. (2019). A numerical investigation on the effects of mixed convection of Ag-water nanofluid inside a sim-circular lid-driven cavity on the temperature of an electronic silicon chip. *Applied Thermal Engineering*, *162*, 114298. https://doi.org/10.1016/j.applthermaleng.2019.114298

Najafabadi, H., & Moraveji, K. (2016). Three-dimensional CFD modeling of fluid flow and heat transfer characteristics of Al2O3/water nanofluid in microchannel heat sink with Eulerian-Eulerian approach. *Iranian Journal of Chemical Engineering (IJChE)*, *13*(4), 46-61. https://doi.org/20.1001.1.17355397.2016.13.4.4.3

Hamilton, R. L., & Crosser, O. K. (1962). Thermal conductivity of heterogeneous two-component systems. *Industrial & Engineering chemistry fundamentals*, *1*(3), 187-191. https://doi.org/10.1021/i160003a005

Heidarshenas, A., Azizi, Z., Peyghambarzadeh, S. M., & Sayyahi, S. (2020). Experimental investigation of the particle size effect on heat transfer coefficient of Al 2 O 3 nanofluid in a cylindrical microchannel heat sink. *Journal of Thermal Analysis and Calorimetry*, *141*, 957-967. https://doi.org/10.1007/s10973-019-09033-7

Ho, C. J., & Chen, W. C. (2013). An experimental study

on thermal performance of Al2O3/water nanofluid in a minichannel heat sink. *Applied Thermal Engineering*, *50*(1), 516-522. https://doi.org/10.1016/j.applthermaleng.2012.07.037

Jawad, M., Khalifa, H. A. E. W., Shaaban, A. A., Akgül, A., Riaz, M. B., & Sadiq, N. (2024a). Characteristics of heat transportation in MHD flow of chemical reactive micropolar nanofluid with moving slip conditions across stagnation points. *Results in Engineering*, *21*, 101954. https://doi.org/10.1016/j.rineng.2024.101954

Jawad, M., Sadiq, N., & Ali, M. R. (2024b). Analysis of chemical reactive tangent hyperbolic nanofluid flow with joule heating and motile microorganisms through stretchable surface. *Bio Nano Science*, *14*(2), 605-618. https://doi.org/10.1007/s12668-023-01268-x

Kahani, M. (2020). Simulation of nanofluid flow through rectangular microchannel by modified thermal dispersion model. *Heat Transfer Engineering*, *41*(4), 377-392. https://doi.org/10.1080/01457632.2018.1540464

Khoshvaght-Aliabadi, M., Hassani, S. M., & Mazloumi, S. H. (2017). Enhancement of laminar forced convection cooling in wavy heat sink with rectangular ribs and Al2O3/water nanofluids. *Experimental Thermal and Fluid Science*, *89*, 199-210. https://doi.org/10.1016/j.expthermflusci.2017.08.017

Kline, S. J. (1963). Describing uncertainties in single-sample experiments. *Mech. Eng.*, *75*, 3-8.

Kulandaivel, S., Ngui, W. K., Samykano, M., Rajamony, R. K., Suraparaju, S. K., Abd Ghafar, N. S., & Mat Noor, M. (2024a). Enhanced heat transfer efficiency through formulation and rheo-thermal analysis of palm oil-based CNP/SiO2 binary nanofluid. *Energy Technology*, *2400314*. https://doi.org/10.1002/ente.202400314

Kulandaivel, S., Samykano, M., Keng, N. W., Rajamony, R. K., Suraparaju, S. K., Sofiah, A. G. N., & Kalidasan, B. (2024b). Nanotechnology Revolutionizing Heat Transfer: A Review of Nanofluid Research and Applications. *Malaysian Journal of Chemistry,* 26(3), 192-210. https://doi.org/10.55373/mjchem.v26i.192

Kumar, P. M., & Kumar, C. A. (2020). Numerical study on heat transfer performance using Al2O3/water nanofluids in six circular channel heat sink for electronic chip. *Materials Today: Proceedings*, *21*, 194-201. https://doi.org/10.1016/j.matpr.2019.04.220.

Kumar, R., Tiwary, B., & Singh, P. K. (2022). Thermofluidic analysis of Al2O3-water nanofluid cooled branched wavy heat sink. *Applied Thermal Engineering*, *201*, 117787. https://doi.org/10.1016/j.applthermaleng.2021.1177

87.

Moghanlou, F. S., Noorzadeh, S., Ataei, M., Vajdi, M., Asl, M. S., & Esmaeilzadeh, E. (2020). Experimental investigation of heat transfer and pressure drop in a minichannel heat sink using Al2O3 and TiO2–water nanofluids. *Journal of the Brazilian Society of Mechanical Sciences and Engineering*, *42*(6), 315. https://doi.org/10.1007/s40430-020-02403-5

Muhammad, N. M. A., Sidik, N. A. C., Saat, A., & Abdullahi, B. (2019). Effect of nanofluids on heat transfer and pressure drop characteristics of diverging-converging minichannel heat sink. *CFD Letters*, *11*(4), 105-120.

Naphon, P., Nakharintr, L., & Wiriyasart, S. (2018). Continuous nanofluids jet impingement heat transfer and flow in a micro-channel heat sink. *International Journal of Heat and Mass Transfer*, *126*, 924-932. https://doi.org/10.1016/j.ijheatmasstransfer.2018.05.101

Naranjani, B., Roohi, E., & Ebrahimi, A. (2021). Thermal and hydraulic performance analysis of a heat sink with corrugated channels and nanofluids. *Journal of Thermal Analysis and Calorimetry*, *146*, 2549-2560. https://doi.org/10.1007/s10973-020-10225-9

Ragueb, H., & Mansouri, K. (2023). Exact solution of the Graetz–Brinkman problem extended to non-Newtonian nanofluids flow in elliptical microchannels. *Journal of Engineering Mathematics*, *140*(1), 10. https://doi.org/10.1007/s10665-023-10267-6

Ragueb, H., Tahiri, A., Behnous, D., Manser, B., Rachedi, K., & Mansouri, K. (2023). Irreversibilities and heat transfer in magnetohydrodynamic microchannel flow under differential heating. *International Communications in Heat and Mass Transfer*, *149*, 107155. https://doi.org/10.1016/j.icheatmasstransfer.2023.107155

Ramasekhar, G., & Jawad, M. (2024). Characteristics of MWCNT, SWCNT, Cu and water based on magnetized flow of nanofluid with Soret and Dufour effects induced by moving wedge: Consequence of Falkner–Skan power law. *Numerical Heat Transfer, Part A: Applications*, 1-15. https://doi.org/10.1080/10407782.2024.2341270

Ramasekhar, G., Divya, A., Jakeer, S., Reddy, S. R. R., Algehyne, E. A., Jawad, M., ... & Hassani, M. K. (2024). Heat transfer innovation of engine oil conveying SWCNTs-MWCNTs-TiO2 nanoparticles embedded in a porous stretching cylinder. *Scientific Reports*, *14*(1), 16448. https://doi.org/10.1038/s41598-024-65740-8

Saadoon, Z. H., Ali, F. H., & Sheikholeslami, M. (2023). Numerical investigation of heat transfer enhancement using (Fe3O4 and Ag-H2O) nanofluids in (converge-diverge) mini-channel heat sinks. *Materials Today: Proceedings*, *80*, 2983-

2996. https://doi.org/10.1016/j.matpr.2021.07.091

Saadoon, Z. H., Ali, F. H., Hamzah, H. K., Abed, A. M., & Hatami, M. (2022). Improving the performance of mini-channel heat sink by using wavy channel and different types of nanofluids. *Scientific Reports*, *12*(1), 9402. https://doi.org/10.1038/s41598-022-13519-0

Sadiq, N., Jawad, M., Khalid, F., Jahan, S., & Hassan, A. M. (2024). Comparative analysis of non-Newtonian and Newtonian fluid flow with dual slip in the presence of motile microorganisms and nanoparticles. *BioNanoScience*, *14*(2), 1504-1519. https://doi.org/10.1007/s12668-023-01284-x

Saeed, M., & Kim, M. H. (2018). Heat transfer enhancement using nanofluids (Al2O3-H2O) in mini-channel heatsinks. *International Journal of Heat and Mass Transfer*, *120*, 671-682. https://doi.org/10.1016/j.ijheatmasstransfer.2017.12.075

Sajid, M. U., Ali, H. M., Sufyan, A., Rashid, D., Zahid, S. U., & Rehman, W. U. (2019). Experimental investigation of TiO2–water nanofluid flow and heat transfer inside wavy mini-channel heat sinks. *Journal of Thermal Analysis and Calorimetry*, *137*(4), 1279-1294. https://doi.org/10.1007/s10973-019-08043-9

Sakanova, A., Keian, C. C., & Zhao, J. (2015). Performance improvements of microchannel heat sink using wavy channel and nanofluids. *International Journal of Heat and Mass Transfer*, *89*, 59-74. https://doi.org/10.1016/j.ijheatmasstransfer.2015.05.033

Sivakumar, A., Alagumurthi, N., & Senthilvelan, T. (2016). Experimental investigation of forced convective heat transfer performance in nanofluids of Al 2 O 3/water and CuO/water in a serpentine shaped micro channel heat sink. *Heat and Mass Transfer*, *52*, 1265-1274. https://doi.org/10.1007/s00231-015-1649-5

Sohel, M. R., Khaleduzzaman, S. S., Saidur, R., Hepbasli, A., Sabri, M. F. M., & Mahbubul, I. M. (2014). An experimental investigation of heat transfer enhancement of a minichannel heat sink using Al2O3–H2O nanofluid. *International Journal of Heat and Mass Transfer*, *74*, 164-172. https://doi.org/10.1016/j.ijheatmasstransfer.2014.03.010

Tahiri, A., Ragueb, H., Moussaoui, M., Mansouri, K., Guerraiche, D., & Guerraiche, K. (2024). Heat transfer and entropy generation in viscous-joule heating MHD microchannels flow under asymmetric heating. *International Journal of Numerical Methods for Heat & Fluid Flow*, *34*(10), 3953-3978. https://doi.org/10.1108/HFF-05-2024-0380

Tang, B., Zhou, R., Bai, P., Fu, T., Lu, L., & Zhou, G. (2017). Heat transfer performance of a novel double-layer mini-channel heat sink. *Heat and Mass Transfer*, *53*, 929-936. https://doi.org/10.1007/s00231-016-1869-3

Tariq, H. A., Anwar, M., & Malik, A. (2020). Numerical investigations of mini-channel heat sink for microprocessor cooling: Effect of slab thickness. *Arabian Journal for Science and Engineering*, *45*(7), 5169-5177. https://doi.org/10.1007/s13369-020-04370-4

Tariq, H. A., Shoukat, A. A., Hassan, M., & Anwar, M. (2019). Thermal management of microelectronic devices using micro-hole cellular structure and nanofluids. *Journal of Thermal Analysis and Calorimetry*, *136*, 2171-2182. https://doi.org/10.1007/s10973-018-7852-0

Waseem, M., Algehyne, E. A., Al-Atawi, N. O., Bognár, G., Jawad, M., & Naeem, S. (2024a). Non-similar analysis of suction/injection and Cattaneo-Christov model in 3D viscoelastic non-Newtonian fluids flow due to Riga plate: a biological applications. *Alexandria Engineering Journal*, *103*, 121-136. https://doi.org/10.1016/j.aej.2024.05.099

Waseem, M., Jawad, M., Naeem, S., & Majeed, A. (2024b). Impact of motile microorganisms and chemical reaction on viscoelastic flow of non-Newtonian fluid with thermal radiation subjected to exponentially stretching sheet amalgamated in Darcy-Forchheimer porous medium. *BioNanoScience*, *14*(2), 1601-1612. https://doi.org/10.1007/s12668-024-01435-8

Waseem, M., Jawad, M., Naeem, S., Bognár, G., Alballa, T., Khalifa, H. A. E. W., ... & Kolsi, L. (2024c). Regression analysis of Cattaneo–Christov heat and thermal radiation on 3D Darcy flow of Non-Newtonian fluids induced by stretchable sheet. *Case Studies in Thermal Engineering*, *61*, 104959. https://doi.org/10.1016/j.csite.2024.104959

Zhang, J., Diao, Y., Zhao, Y., & Zhang, Y. (2017). An experimental investigation of heat transfer enhancement in minichannel: Combination of nanofluid and micro fin structure techniques. *Experimental Thermal and Fluid Science*, *81*, 21-32. https://doi.org/10.1016/j.expthermflusci.2016.10.001